Journal of Functional Materials and Applied Engineering

Research Paper

Process optimization of tetracycline degradation by H2O2

Burker Ooi[1], Pietro NG Buono[2,*], Sonia Viknesh[1], Aimin Lanzalaco[1], Christian Sirés[1]

[1] Department of Chemical Sciences, University of Padua, 35131 Padova, Italy
[2] Departament d'Enginyeria Química, EEBE, Universitat Politècnica de Catalunya, 08019 Barcelona, Spain
*Corresponding author: p.buono@ub.edu

Abstract. Antibiotic abuse has evolved into a serious and pressing global concern. The misuse of antibiotics has precipitated a range of problems, particularly posing significant threats to aquatic environments. Antibiotic contamination in water bodies leads to the persistence of antibiotics and their metabolites, causing toxic influences and harm to aquatic organisms, damaging genetic and cellular structures, and contributing to the escalation of bacterial resistance. Consequently, addressing antibiotic pollution in aquatic systems is paramount for safeguarding water quality and ecological balance. For edta-Fe^o/H2O2 system, using 0.3 g/L edta-Fe^o and 60mm H2O2, under the condition of pH 6.5, TC can be influenceively removed within 60 minutes, and the removal rate can reach 90.2%. In contrast, the unmodified FE^o/H2O2 system can only remove 23.9% of TC. In addition, edta-Fe^o/H2O2 system has good removal influence on different types of pollutants, and has good recycling capacity and adaptability, which is suitable for actual wastewater treatment. Through quenching test EPR, the catalytic mechanism of edta-Fe^o for H2O2 was confirmed by the studies of shell separated nano particle enhanced Raman spectroscopy (shiners) and DFT calculation, and · oh was found to be the main reaction species. Therefore, enhancing the decomposition of H2O2 to produce · OH plays an important role in enhancing the degradation of pollutants. H2O2 can be decomposed in two ways, namely, the breaking of peroxide bond to form · OH or the breaking of O-H bond to form *ooh. Then, the peroxide bond breaks and · OH is produced by impact. EDTA-Fe^o modification can enhance these decomposition pathways, so as to produce more · OH and improve the catalytic activity. The reaction path and intermediate products of edta-Fe^o/H2O2 were detected by LC-MS. toxicity evaluation showed that the toxicity of TC was reduced. In addition, the structure, in particular functional groups, of APCA on performance of APCA-Fe^o system was explored. The amount of carboxyl group (-COOH) is very important to improve the performance, and amino (-NH2) group content also plays a role in the performance of APCA-Fe^o system. When catalyst contains more COOH and NH2 groups, the reaction activity and antibiotic elimination rate will be improved. The synergistic influence of NH2 and COOH groups can promote electron transfer and accelerate Fe (II) liberation, thus enhancing the performance and TC removal. Therefore, in design and preparation of APCA-Fe^o, selecting the appropriate APCA can enhance permeability of the catalyst, so as to improve its performance and application value.

Keywords: *Tetracycline; Hydrogen peroxide; Antimicrobial removal*

Received on 21 June 2024, Accepted on 30 August 2024, Published on 15 September 2024

1 Introduction

Antibiotic is a class of drugs which can inhibit or kill bacteria and are widely used in clinical treatment for various bacterial infections. However, irrational use and overuse of antibiotics have become a serious issue. China is one of the world's largest consumers of antibiotics, with usage remaining consistently high [1]. Due to its large population and significant disease burden, many patients tend to use antibiotics for various infections, even for minor colds. This irrational use leads to persistently high consumption levels, making antibiotic abuse an increasingly prominent problem. Firstly, antibiotic residues and pollution are significant concerns. In agriculture, antibiotics are widely used to prevent and treat animal diseases, subsequently entering the environment through manure [2]. Residual antibiotics may enter the human food chain via crops and water sources, increasing human exposure and posing potential health threats [3]. Furthermore, antibiotic use can promote the development of bacterial resistance. The existance of antibiotics in the environment can lead bacteria to acquire resistance genes, increasing antibiotic resistance and making infections harder to treat [4]. The

development of antibiotic resistance not only challenges healthcare but also impacts microbial communities and ecosystem stability [5].

Antibiotics, widely used in healthcare and aquaculture, are partially excreted by humans, animals, and plants into the water environment, causing a series of hazards. Firstly, antibiotic pollution leads to the persistence of residues and their metabolites [6]. During treatment, some drugs are not fully absorbed and enter water bodies via excrement, causing contamination. These residues can persist for long periods, are difficult to degrade, and not only affect water quality and ecosystems but also pose bioaccumulation risks. Secondly, antibiotic residues are toxic and harmful to aquatic life. Many antibiotics are toxic to organisms like fish, algae, and plankton at certain concentrations. Prolonged exposure can cause abnormal growth, weakened immunity, reduced reproductive capacity, and even death [7]. Thirdly, antibiotic residues can damage the genetic and cellular structures of aquatic organisms, further affecting biodiversity and ecological balance [8]. Fourthly, they can promote bacterial resistance [1, 9]. While antibiotics inhibit or kill bacteria, their presence in the environment can lead to resistant bacterial strains. These strains can spread through water to seafood, food, and even humans, increasing treatment difficulties and threatening public health [9]. Finally, antibiotic pollution can facilitate horizontal gene transfer among bacteria in water bodies [10]. Interaction between antibiotic residues and bacteria can promote the spread of resistance genes, exacerbating antibiotic resistance [10].

H_2O_2-based AOPs are efficient and environmentally friendly [11]. Common systems include UV/H_2O_2, H_2O_2/O_3, and Fenton reactions. UV/H_2O_2: UV radiation cleaves H_2O_2, producing •OH radicals that influenceively degrade pollutants [12]. However, high H_2O_2 concentrations can scavenge •OH, requiring careful optimization. O_3/H_2O_2: This combination promotes •OH generation via a radical chain mechanism initiated by the conjugate base of H_2O_2 (HO_2^-) [13]. It enhances the degradation and mineralization of pollutants like ofloxacin compared to ozone alone [14]. Fenton and Fenton-like Reactions: The classic Fenton reaction uses Fe^{2+} and H_2O_2 to generate •OH under acidic conditions (pH 3-5) [14]. It influenceively oxidizes various organics but produces iron sludge and has a narrow pH range. Fenton-like reactions use other catalysts or energy sources (e.g., UV, visible light) to overcome limitations [15]. Pretreatment of FE^o (e.g., pre-magnetization) [16] or adding chelating agents (e.g., EDTA) [16] can enhance performance at neutral pH.

FE^o-based AOPs are environmental remediation technologies that use FE^o particles to transform organic and inorganic pollutants into less toxic or harmless substances via redox reactions [17]. FE^o is influenceive, inexpensive, and easy to use. It can treat multiple pollutants simultaneously and is environmentally friendly [18]. Applications include groundwater remediation, wastewater treatment, and soil remediation [19].

Despite its potential, FE^o technology faces challenges, primarily passivation and agglomeration [20]. Passivation occurs when $Fe(OH)_2$ and $Fe(OH)_3$ form a layer on the FE^o surface, hindering contact with pollutants and reducing reactivity [21]. Iron also oxidizes in air, forming an oxide film [21]. Agglomeration, especially for nano-FE^o due to high surface energy and magnetism, leads to larger particles, reduced surface area, and lower reactivity [22]. It also complicates separation and recovery [23]. Strategies to address these include using modifiers, stabilizers, or surface functionalization [24].

This study modifies Fe^o using a liquid-phase impregnation method with EDTA, a typical APCA containing 4 carboxyl and 2 amino groups. It constructs two catalytic systems: EDTA-Fe^o/PAA and EDTA-Fe^o/H_2O_2. Using typical antibiotics SMT and TC as target pollutants, it investigates the influences of modification parameters, system dosage, initial pH, and coexisting anions, revealing the enhanced activation mechanism of EDTA-FE^o. It also selects different APCAs (EDTA, NTA, BTCA) to modify Fe^o, exploring influence of structureon performance of APCA and characterization of APCA-Fe^o system. Specific research contents included: (1) Efficiency and Mechanism of Antibiotic Degradation by EDTA-Fe^o/H_2O_2 and EDTA-Fe^o/PAA Systems. (2) Study on the Catalytic Mechanism of EDTA-Fe^o Enhanced Oxidant Activation. (3) Study on the relationship between APCA structure and APCA-Fe^o performance.

2 Materials and Methods

2.1 Materials

All chemicals and reagents used were of analytical grade, such as ferric nitrate ($Fe(NO_3)_3 \cdot 6H_2O$), cobalt nitrate ($Co(NO_2)_3 \cdot 6H_2O$), ammonium fluoride (NH_4F), urea ($CO(NH_2)_2$), hydrochloric acid (HCl), NaOH, sodium hypophosphite, tert-butyl alcohol (TBA), p-benzoquinone, and 1,10-Phenanthroline monohydrate. Nickel foam (NF) (thickness 1.0 mm, 300 g m^{-2}) was purchased from Taobao, China. Tetracycline hydrochloride was purchased from Sinopharm Chemical Reagent Co., Ltd. The ultrapure water used had a resistivity of 18.25 MΩ·cm.

2.2 Degradation Experiments and Analytical Methods

In the degradation experiments, a 500 mL solution of 50 mM TC was prepared in a beaker and experiments were conducted at ambient temperature. Firstly, 0.1 M NaOH or HCl solution was used to adjust the starting pH of the TC solution of 6.5. Subsequently, stirring was initiated using an electric stirrer at a speed of 360 rpm. The catalyst (Fe^o/EDTA-Fe^o) and oxidant (H_2O_2) were added to the stirring TC solution to start the antibiotic degradation process. Samples were taken at specific time intervals; 500 μL of methanol was added to 1 mL of sample to quench the reaction. Finally, the samples passed through 0.22 μm membrane for further analysis.

Influence of other factors on the reaction was investigated, including EDTA-FE^o dosage (0.05-0.3 g/L), initial pH (3, 5, 6.5, 8, 9.5), addition of 1-10 mM inorganic ions and humic acid (Cl^-, SO_4^{2-}, NO_3^-, HCO_3^-, HA), and background water quality. Furthermore, to assess the role of radicals, inhibitors such as 1 M TBA, 1 M MeOH, and 5 mM 2,4-HD were added to the experiments.

2.3 Characterization Methods

A Thermo Fisher Nexsa X-ray photoelectron spectrometer was used to conduct an in-depth analysis of the composition, oxidation state, and content of key elements, including Fe and O, in the APCA-Fe^o.

To deeply investigate the microscopic surface changes of FE^o and EDTA-FE^o during chemical reactions, high-precision observations were carried out using a German Zeiss Sigma 300 scanning electron microscope. By observing FE^o and EDTA-FE^o samples before and after the reaction with SEM, precise morphological evolution of these two materials during the reaction process was obtained, providing a scientific basis for optimizing material performance and enhancing reaction efficiency.

FTIR spectroscopy was used to identify functional groups on material surfaces. Surface chemical characteristics of EDTA-FE^o and Fe^o were thoroughly studied using a Thermo Scientific Nicolet iS20 infrared spectrometer.

The surface contact angle of the materials was measured using a JC2000DM precision contact angle measuring instrument. By measuring the contact angle of multiple droplets on the sample surface and statistically analyzing the results, the surface hydrophilicity/hydrophobicity characteristics of the materials were determined.

Raman spectra were measured with a 633 nm excitation laser source (power at 10% of the source power).

Tafel curves were analyzed using an electrochemical workstation (CHI760E). A platinum counter electrode, a saturated calomel electrode, counter electrode, and working electrode, respectively. All electrodes were immersed in a 0.1 M Na_2SO_4 solution. The scan rate was 1 mV/s.

2.4 Measurements

TC concentration was measured by UV-visible spectra at 357 nm.

TC elimination rate (%) was calculated using Equations (1).

$$\eta = (1 - \frac{C_t}{C_0}) * 100\% \quad (1)$$

Constant (k /min^{-1}) of Pseudo first order model was calculated following Equations (2).

$$k_{\mathrm{obs}} = \ln \frac{C_t}{C_0} \quad (2)$$

The 1,10-phenanthroline spectrophotometric method was used to determine dissolved Fe^{2+} and total iron concentrations. This method is based on the principle that Fe^{2+} forms a stable orange-red complex with 1,10-phenanthroline under acidic conditions. First, the test solution was filtered to remove impurities. Then, an acetate-acetic acid buffer solution and 1,10-phenanthroline solution were added, mixed thoroughly, and left to stand for 15 minutes. Afterwards, absorbance was detected by UV-Vis spectrophotometer at wavelength of 510 nm. To determine concentration of total iron, a hydroxylamine hydrochloride solution was added first to reduce all dissolved iron to the Fe^{2+} state, followed by the same procedure. By measuring the absorbance and using a standard curve or calculation formula, the quantitative results for Fe^{2+} or total iron concentration can be obtained. This method accurately determines dissolved Fe^{2+} and total iron concentrations, aiding in the analysis and control of iron content in samples.

BA (benzoic acid) is converted to p-HBA (p-hydroxybenzoic acid) upon reaction with ·OH, and the concentration of p-HBA can be accurately determined by HPLC. The concentration of ·OH was further calculated based on the quantitative relationship shown in Equation (3).

$$c(\cdot OH)=[pHBA]\times 5.87 \quad (3)$$

For the determination of Fe(IV) generated, methyl phenyl sulfoxide (PMSO) was used as probe. Reaction is between Fe(IV) and PMSO, generating $PMSO_2$ (methyl phenyl sulfone). The amount of $PMSO_2$ generated was precisely measured by HPLC, and the Fe(IV) content was accurately calculated based on the quantitative relationship. To measure Fe(IV), 0.5 mL of dimethyl sulfoxide was first added to a centrifuge tube to quench the reaction. Then, at specified time intervals, 1 mililiter of reaction solution was pipetted into a tube. To ensure sample purity, the sample was filtered by 0.22 μm organic membrane. Finally, the processed sample was analyzed under the corresponding liquid chromatography conditions to precisely determine the Fe(IV) content in the system.

DMPO (5,5-dimethyl-1-pyrroline N-oxide) was used as a spin trap for ·OH. Tests were conducted using an EPR spectrometer (Bruker ELEXSYS 580). The test conditions were as follows: center field: 3518.65 G; microwave frequency: 9.85 GHz; microwave power: 2.00 mW; modulation amplitude: 0.9 G; frequency: 100 kHz; time constant: 0.01 ms; sweep width: 180 G; sweep time: 25 s.

Structural models of Fe^0 and EDTA-Fe^0 were constructed. The degradation pathways of H_2O_2 and the Gibbs free energy under Fe^0 and EDTA-Fe^0 catalysis were determined using VASP calculations. The adsorption energies of H_2O_2 and *OOH on Fe^0 and EDTA-Fe^0, as well as the adsorption energy and free energy of PAA adsorption on Fe^0 and EDTA-Fe^0, were also calculated.

The toxicity of TC, SMT, degradation intermediates was evaluated using the Toxicity Estimation Software Tool (T.E.S.T.). The mutagenicity, toxicity, Tetrahymena pyriformis IGC50 (48 h), and fathead minnow LC50 (96 h) of the organic compounds were used as indicators.

3 Results and Discussion

3.1 Influence of EDTA Concentration on EDTA-Fe^0

The amount of EDTA used during modification significantly affects the reactivity of EDTA-Fe^0. As shown in Fig. 1(a) and Fig. 1(b), the introduction of EDTA significantly improved the efficiency of TC removal by Fe^0. Further analysis revealed that the reaction system with EDTA-FE^0 prepared using 0.2 M EDTA had a rate constant kof 0.035 min^{-1}, which is much higher than the rate constants at other EDTA concentrations: 0.018 min^{-1} at 0.1 M

EDTA, 0.029 min^{-1} at 0.3 M EDTA, and 0.023 min^{-1} at 0.4 M EDTA. Based on these results, an EDTA concentration of 0.2 M was selected for preparing EDTA-FE^0.

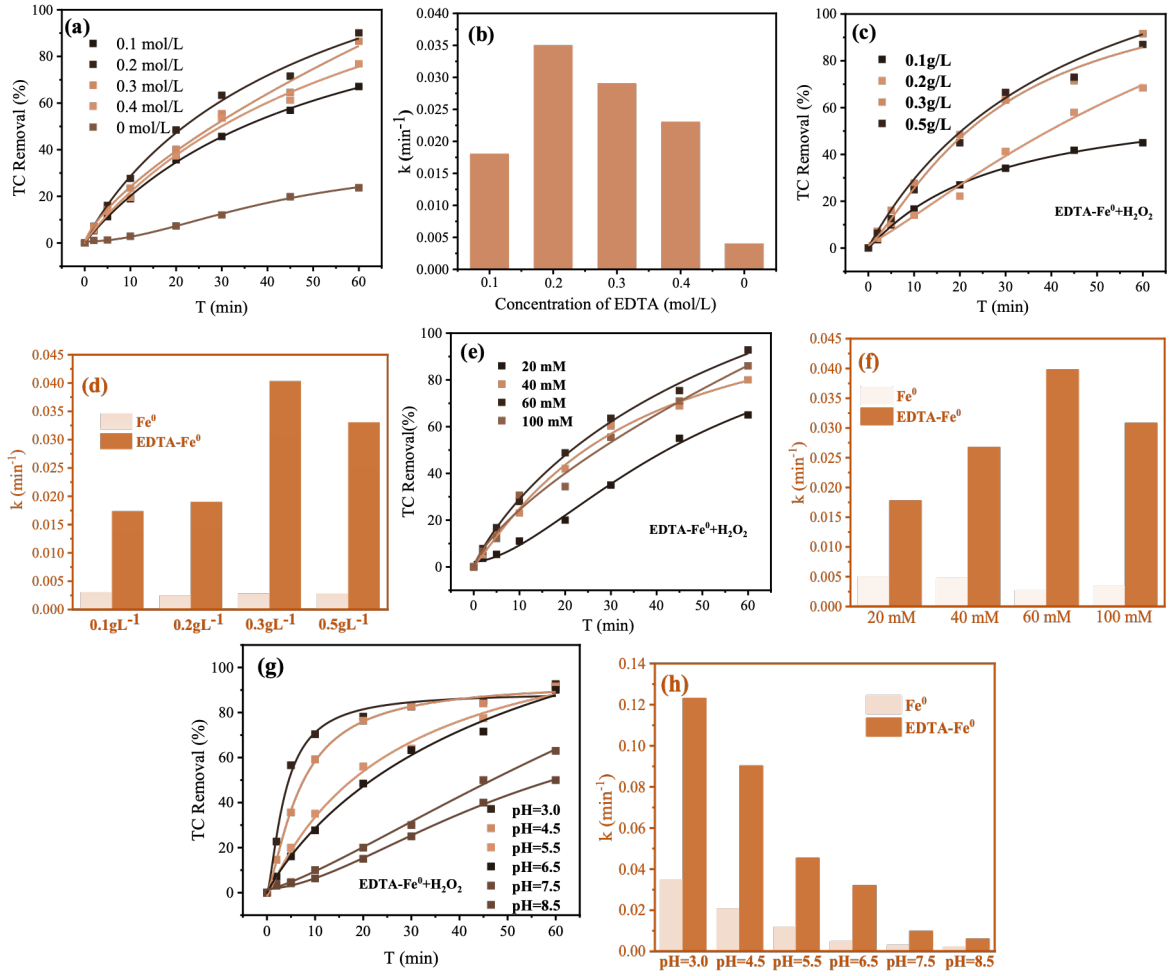

Figure 1 (a) Influence of EDTA concentrations on TC removal; (b) k value at various EDTA concentrations; (c) Influence of EDTA-Fe^0 dosages on removal rate; (d) k value at different dosages; (e) Influence of H_2O_2 dosages on TC removal; (f) k value ; (g) influence of pH on TC removal; (h) k value at different pH

3.2 Influence of EDTA-FE^0 Dosage

As in Fig. 2(a), Fig. 1(c), and Fig. 1(d), the TC elimination rate increased notably when the EDTA-Fe^0 concentration raised to 0.3 g/L. In aprticular, elimination rate enhance markedly from 46.88% to 93.23 %. Concurrently, the k_{value} increased from 0.016 min^{-1} to 0.044 min^{-1}. When the EDTA-FE^0 was further increased to 0.5 g/L, a marginal decrease in TC elimination to 86.58 % was shown, with a reduction in the kvalue to 0.031 min^{-1}. This reduction mainly ascribed to the existance of excessive EDTA-FE^0, leading to an overabundance of dissolved iron which might inhibit the reactivity of ·OH radicals. Further, the kvalue for with 0.3 g/L EDTA-FE^0/H_2O_2 was 0.027 min^{-1}, which is 13.7 times higher than that of the FE^0/H_2O_2 system. Therefore, the EDTA-FE^0/H_2O_2 system demonstrated superior performance in terms of both TC elimination rate and stable reaction rate. These results indicate that an appropriate amount of EDTA-FE^0 can enhance TC removal rate and degradation efficiency, but an excess may lead to over-reaction. Thus, optimizing the EDTA-FE^0 concentration is necessary for achieving optimal degradation in practical applications.

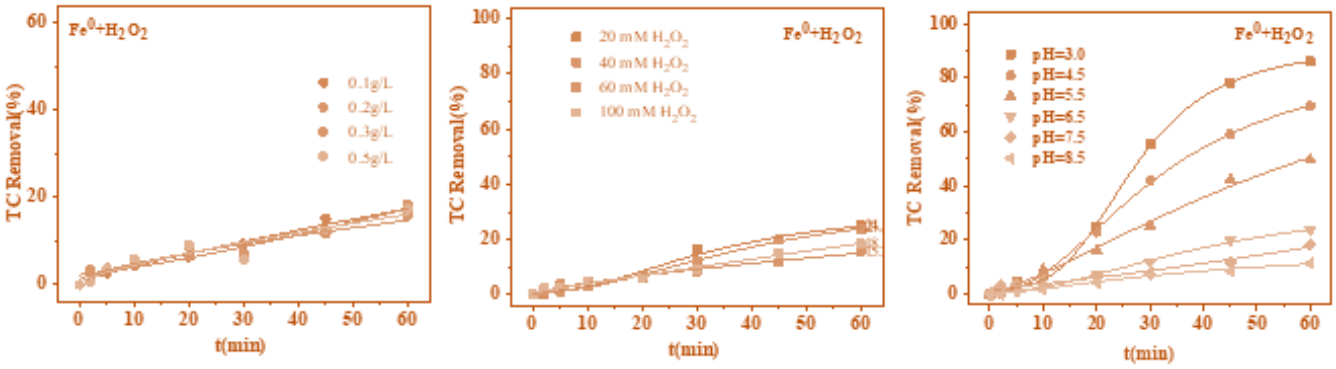

Figure 2 (a) The elimination rate of TC at different dosage of Fe^0/H_2O_2 ; (b) the elimination rate of TC at different dosage of H_2O_2 in FE^0/H_2O_2; (c) the elimination rate of TC at different pH in Fe^0/H_2O_2

3.3 Influence of H_2O_2 Dosage

As seen in Fig. 2(b), Fig. 1(e), and Fig. 1(f), the influence of H_2O_2 concentration on TC elimination rate in the EDTA-Fe^0/H_2O_2 system can be clearly observed. When the H_2O_2 concentration increased from 20 mM to 60 mM, the TC elimination rate showed a significant upward trend, increasing from 66.1% to 91.2%. Simultaneously, the reaction rate constant kincreased from 0.017 min^{-1} to 0.040 min^{-1}, indicating an acceleration of the reaction rate with increasing H_2O_2 concentration. However, when the H_2O_2 concentration was further increased to 100 mM, the TC elimination rate decreased to 86.2%, and the reaction rate constant decreased to 0.030 min^{-1}. This change occurs because excess H_2O_2 can react with the reactive radicals in the system, thereby consuming the oxidant originally intended for TC degradation. Additionally, excess H_2O_2 might adsorb onto the surface of EDTA-Fe^0, hindering its dissolution and further reaction, leading to a reduction in the overall system reactivity. Nevertheless, regardless of the H_2O_2 concentration variation, the EDTA-Fe^0/H_2O_2 system proved higher elimination rate and reaction rate compared to the conventional Fe^0/H_2O_2 system. Specifically, at an H_2O_2 dose of 60 mM, the TC elimination rate using the EDTA-Fe^0/H_2O_2 system was as high as 92.11%, with a kvalue of 0.040 min^{-1}. In contrast, the conventional Fe^0/H_2O_2 system performed poorly under the same conditions, achieving only 15.3% TC removal and a kvalue of 0.0026 min^{-1} at the same H_2O_2 dose. This comparative data further emphasizes the superiority of the EDTA-FE^0/H_2O_2 system for TC degradation and indicates that, besides improving elimination rate and reaction rate, it also helps reduce H_2O_2 consumption.

3.4 Influence of Initial pH

As shown in Fig. 2(c), Fig. 1(g), and Fig. 1(h), the EDTA-Fe^0/H_2O_2 system showed better TC elimination rate under acidic pH conditions. As the initial pH increased, the TC elimination rate gradually decreased. However, in the EDTA-Fe^0/H_2O_2 system, the TC removal rate still reached 90.2% even at neutral pH. This result indicates that the system remains influenceive in a neutral environment, demonstrating a broad pH applicability range. Furthermore, compared to the Fe^0/H_2O_2 system, the kvalue in the EDTA-Fe^0/H_2O_2 system was enhanced by 2.8 to 14.4 times across different pH levels. The results demonstrate that, compared to conventional Fe^0, EDTA-Fe^0 can broaden the applicable pH range for the H_2O_2-based system.

3.5 Influence of Coexisting Anions and Humic Acid

Inorganic ions and natural organic matter are ubiquitous components in wastewater and significantly impact TC removal. The system's resistance to ions was tested using HCO_3^- and NO_3^- at concentrations of 0.2 mM, 0.5 mM, 1 mM, and 2 mM; SO_4^{2-} and Cl^- at 1 mM, 5 mM, 10 mM, and 20 mM; and HA at 2 mg/L, 5 mg/L, 10 mg/L, and 20 mg/L. Experimental results in Fig. 3 show that various inorganic ions affected TC removal to some extent. Among them, SO_4^{2-} and Cl^- slightly increased the H_2O_2 decomposition rate, primarily because they can enhance the corrosion rate of EDTA-Fe^0, increasing the number of reduction sites on its surface, thereby accelerating TC removal [25-26]. Additionally, the presence of HA in the solution forms soluble humic acid-iron complexes, inhibiting the passivation of EDTA-Fe^0 and the precipitation of iron corrosion products [27], thus promoting TC removal. Conversely, HCO_3^- and NO_3^- significantly inhibited TC removal [28]. This is because they can react with ·OH to form HCO_3· that is less reactive and NO_3· radicals [29], leading to poorer degradation kinetics

(Equations (4) and (5)). Comparative experiments revealed that EDTA-Fe^{o} outperformed other modified Fe^{o} reagents in terms of TC elimination rate [30]. The natural organic matter and inorganic ions present in water have varying influences on TC removal. Therefore, understanding these influences is crucial for optimizing the EDTA-Fe^{o}/H_2O_2 system to influenceively degrade TC.

$$\cdot OH + HCO_3^- \rightarrow OH^- + HCO_3 \cdot \quad (4)$$

$$\cdot OH + NO_3^- \rightarrow OH^- + NO_3 \cdot \quad (5)$$

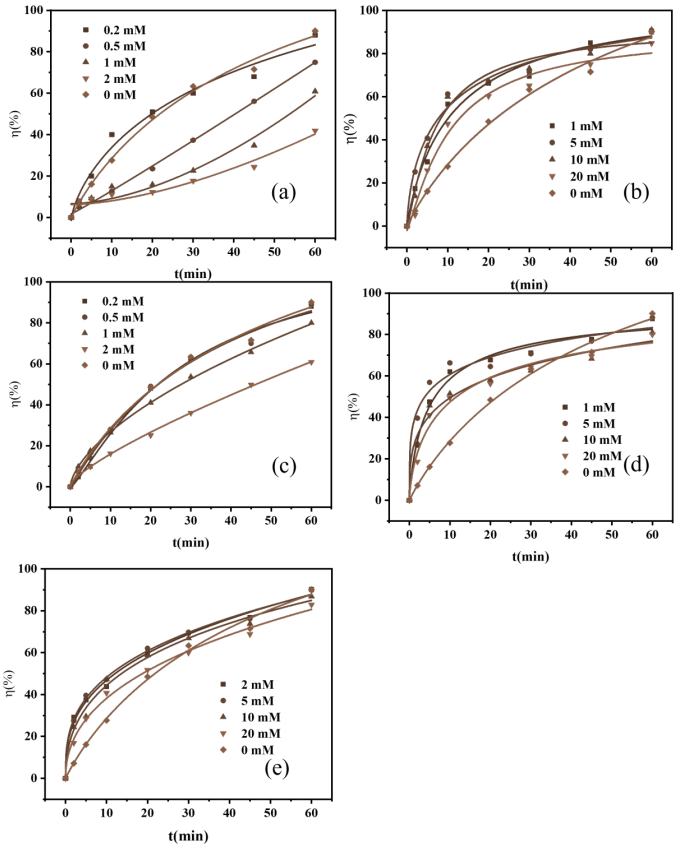

Figure 3 Influence of coexisting inorganic ions on the TC removal in EDTA-FE^{o}//H_2O_2 a) HCO_3^-b) SO_4^{2-} c) NO_3^-d) Cl^- e) humic acid. Reaction condition: [TC] 50 mg/L, [pH] 6.5, [H_2O_2] 60 mM, and [EDTA-FE^{o}] 0.3 g/L

4 Conclusions

In EDTA-Fe^0/H_2O_2 system, · OH is the dominant reaction species. And we found that H_2O_2 can be decomposed in two ways: one is the formation of · OH through the fracture of O-O bond, and the other is the formation of excited state *OOH through the fracture of O-H bond, thus producing · OH. EDTA-ZVI can simultaneously enhance these decomposition pathways, thus producing more · OH, thereby improving the catalytic activity.

The intermediate products of EDTA-Fe^0/H_2O_2 system were detected by LC-MS, and their mutagenicity, LC50 toxicity and developmental toxicity were evaluated. It was confirmed that the intermediate formation in EDTA-Fe^0/H_2O_2 system could reduce the toxicity of target pollutant TC.

The structure of APCA group has a clear relationship with the performance of APCA-Fe^0. The more the number of COOH and NH_2 groups, the better the reactivity of APCA-Fe^0 system. Therefore, in the design of APCA-Fe^0

system, selecting the appropriate combination of APCA is the key, which can help to optimize the permeability of catalyst, improve its performance and application value.

References

[1] Zhao Z, Dong W, Wang H, et al. Advanced oxidation removal of hypophosphite by O3/H2O2 combined wit h sequential Fe(II) catalytic process [J]. Chemosphere, 2017, 180: 48-56.

[2] Zhao F, Yang L, Chen L, et al. Bioaccumulation of antibiotics in crops under long-term manure application: Occurrence, biomass response and human exposure [J]. Chemosphere, 2019, 219: 882-95.

[3] Matsumoto M, Wada Y, Matsumiya S, et al. Enhanced generation of active oxygen species induced by O3 fine bubble injection under H2O2 addition and UV irradiation [J]. Ozone: Science & Engineering, 2021, 43 (6): 562-70.

[4] Omotola E O, Genthe B, Ndlela L, et al. Evaluation of the probable synergistic toxicity of selected potentia ted antiretroviral and antibiotics on some aquatic biomarker organisms [J]. Environmental Monitoring an d Assessment, 2023, 195(12): 1489.

[5] Hernandez-Beltran J C R, Rodríguez-Beltrán J, Aguilar-Luviano O B, et al. Plasmid-mediated phenotypic noi se leads to transient antibiotic resistance in bacteria [J]. Nature Communications, 2024, 15(1): 2610.

[6] Wang X, Jing J, Zhou M, et al. Recent advances in H2O2-based advanced oxidation processes for removal of antibiotics from wastewater [J]. Chinese Chemical Letters, 2023, 34(3): 107621.

[7] Keen O S, Linden K G. Degradation of Antibiotic Activity during UV/H2O2 Advanced Oxidation and Photoly sis in Wastewater Effluent [J]. Environmental Science & Technology, 2013, 47(22): 13020-30.

[8] Ferro G, Guarino F, Castiglione S, et al. Antibiotic resistance spread potential in urban wastewater effluen ts disinfected by UV/H2O2 process [J]. Science of The Total Environment, 2016, 560-561: 29-35.

[9] Nguyen C H, Tran M L, Van Tran T T, et al. Efficient removal of antibiotic oxytetracycline from water by Fe nton-like reactions using reduced graphene oxide-supported bimetallic Pd/nZVI nanocomposites [J]. Jour nal of the Taiwan Institute of Chemical Engineers, 2021, 119: 80-9.

[10] Luo L, Huang W, Zhang J, et al. Metal-Based Nanoparticles as Antimicrobial Agents: A Review [J]. ACS Appl ied Nano Materials, 2024, 7(3): 2529-45.

[11] Kayan I, Oz N A, Kantar C. Comparison of treatability of four different chlorophenol-containing wastewate r by pyrite-Fenton process combined with aerobic biodegradation: Role of sludge acclimation [J]. Journal of Environmental Management, 2021, 279: 111781.

[12] Martin-Laurent F, Topp E, Billet L, et al. Environmental risk assessment of antibiotics in agroecosystems: e cotoxicological influences on aquatic microbial communities and dissemination of antimicrobial resistanc es and antibiotic biodegradation potential along the soil-water continuum [J]. Environmental Science and Pollution Research, 2019, 26(18): 18930-7.

[13] Nnadozie C F, Odume O N. Freshwater environments as reservoirs of antibiotic resistant bacteria and thei r role in the dissemination of antibiotic resistance genes [J]. Environmental Pollution, 2019, 254: 113067.

[14] Xiao X, Sun Y, Sun W, et al. Advanced treatment of actual textile dye wastewater by Fenton-flocculation p rocess [J]. The Canadian Journal of Chemical Engineering, 2017, 95(7): 1245-52.

[15] Hermosilla D, Cortijo M, Huang C P. Optimizing the treatment of landfill leachate by conventional Fenton and photo-Fenton processes [J]. Science of The Total Environment, 2009, 407(11): 3473-81.

[16] Pisharody L, Gopinath A, Malhotra M, et al. Occurrence of organic micropollutants in municipal landfill lea chate and its influenceive treatment by advanced oxidation processes [J]. Chemosphere, 2022, 287: 1322 16.

[17] Changotra R, Rajput H, Dhir A. Treatment of real pharmaceutical wastewater using combined approach of Fenton applications and aerobic biological treatment [J]. Journal of Photochemistry and Photobiology A: Chemistry, 2019, 376: 175-84.

[18] Wu Y, Guan C-Y, Griswold N, et al. Zero-valent iron-based technologies for removal of heavy metal(loid)s and organic pollutants from the aquatic environment: Recent advances and perspectives [J]. Journal of Cl eaner Production, 2020, 277: 123478.

[19] Lu H-J, Wang J-K, Ferguson S, et al. Mechanism, synthesis and modification of nano zerovalent iron in wat er treatment [J]. Nanoscale, 2016, 8(19): 9962-75.

[20] Verma M, Haritash A K. Degradation of amoxicillin by Fenton and Fenton-integrated hybrid oxidation proc esses [J]. Journal of Environmental Chemical Engineering, 2019, 7(1): 102886.

[21] Huang T, Zhang G, Zhang N, et al. Pre-magnetization by weak magnetic field enhancing Fe0-Fenton proces s for wastewater treatment [J]. Chemical Engineering Journal, 2018, 346: 120-6.
[22] Wu Y, Zhu J-y, Bai J-w, et al. The ability of pre-magnetized zero-valent iron for peroxymonosulfate activati on to remove ofloxacin [J]. Chemical Engineering Journal, 2023, 461: 141825.
[23] Zhang Y, Zhou M. A critical review of the application of chelating agents to enable Fenton and Fenton-like reactions at high pH values [J]. Journal of Hazardous Materials, 2019, 362: 436-50.
[24] Rodríguez R, Espada J J, Pariente M I, et al. Comparative life cycle assessment (LCA) study of heterogeneo us and homogenous Fenton processes for the treatment of pharmaceutical wastewater [J]. Journal of Cle aner Production, 2016, 124: 21-9.
[25] Chen H, Wang J. Degradation and mineralization of ofloxacin by ozonation and peroxone (O3/H2O2) proc ess [J]. Chemosphere, 2021, 269: 128775.
[26] Jiang Y, Ran J, Mao K, et al. Recent progress in Fenton/Fenton-like reactions for the removal of antibiotics in aqueous environments [J]. Ecotoxicology and Environmental Safety, 2022, 236: 113464.
[27] Huang X, Chen P, Shi J, et al. Natural substance-mediated synthesis for biochar-supported nanoscale zero-valent iron enhanced the performance of the catalytic process [J]. Materials Today Sustainability, 2023, 2 3: 100461.
[28] Zhu N, Ji H, Yu P, et al. Surface Modification of Magnetic Iron Oxide Nanoparticles [J]. Nanomaterials, 201 8, 8(10): 810.
[29] Zhu Y, Li H, Zhang G, et al. Removal of hexavalent chromium from aqueous solution by different surface-m odified biochars: Acid washing, nanoscale zero-valent iron and ferric iron loading [J]. Bioresource Technol ogy, 2018, 261: 142-50.
[30] Liang Y, Min X, Chai L, et al. Stabilization of arsenic sludge with mechanochemically modified zero valent i ron [J]. Chemosphere, 2017, 168: 1142-51.